

DOI: 10.1002/cbic.200800219

# Identification of Additional Players in the Alternative Biosynthesis Pathway to Isovaleryl-CoA in the Myxobacterium *Myxococcus xanthus*

Helge B. Bode,<sup>[a]</sup> Michael W. Ring,<sup>[a]</sup> Gertrud Schwär,<sup>[a]</sup> Matthias O. Altmeyer,<sup>[a]</sup> Carsten Kegler,<sup>[a]</sup> Ivy R. Jose,<sup>[b]</sup> Mitchell Singer,<sup>[b]</sup> and Rolf Müller<sup>\*,[a]</sup>

*Isovaleryl-CoA (IV-CoA) is usually derived from the degradation of leucine by using the Bkd (branched-chain keto acid dehydrogenase) complex. We have previously identified an alternative pathway for IV-CoA formation in myxobacteria that branches from the well-known mevalonate-dependent isoprenoid biosynthesis pathway. We identified 3-hydroxy-3-methylglutaryl-CoA (HMG-CoA) synthase (MvaS) to be involved in this pathway in Myxococcus xanthus, which is induced in mutants with impaired leucine degradation (e.g., bkd<sup>-</sup>) or during myxobacterial fruiting-body formation. Here, we show that the proteins required for leucine degradation are also involved in the alternative IV-CoA biosynthesis pathway through the efficient catalysis of the reverse*

*reactions. Moreover, we conducted a global gene-expression experiment and compared vegetative wild-type cells with bkd mutants, and identified a five-gene operon that is highly up-regulated in bkd mutants and contains mvaS and other genes that are directly involved in the alternative pathway. Based on our experiments, we assigned roles to the genes required for the formation of IV-CoA from HMG-CoA. Additionally, several genes involved in outer-membrane biosynthesis and a plethora of genes encoding regulatory proteins were decreased in expression levels in the bkd<sup>-</sup> mutant; this explains the complex phenotype of bkd mutants including a lack of adhesion in developmental submerge culture.*

## Introduction

Leucine is not only one of the major amino acids in proteins, but it is also essential for the growth of the myxobacterium *Myxococcus xanthus*.<sup>[1]</sup> *M. xanthus* is a predatory organism and feeds on other bacteria and fungi; therefore leucine is not expected to be in short supply during growth. Amino acid starvation results in the induction of the developmental life cycle including myxospore formation, which allows the species to survive harsh conditions.<sup>[2]</sup> Leucine is also important for *M. xanthus* because leucine-derived iso-branched fatty acids (FAs) represent the dominant FAs in *M. xanthus* and myxobacteria in general.<sup>[3–7]</sup> The biosynthesis of these iso-FAs in myxobacteria requires isovaleryl-CoA (IV-CoA) as starting unit. IV-CoA is usually derived from the transamination of leucine to 2-ketoisocaproic acid and subsequent oxidative decarboxylation to IV-CoA by the Bkd complex, which is also involved in the degradation of valine and isoleucine.<sup>[8]</sup> A reduction of the amount of iso-FAs (e.g., in *bkd* mutants) results in delayed aggregation and reduced myxospore formation under starvation conditions in *M. xanthus*.<sup>[7,9,10]</sup> This developmental phenotype can be explained by the fact that iso-FA-derived etherlipids are specifically produced within the myxospore and seem to represent the dominant lipids in mature myxospores.<sup>[10]</sup> In addition to the proposed structural function(s) of leucine-derived lipids it cannot be excluded that signals derived from iso-FAs play a role in myxobacterial fruiting-body formation as previously suggested.<sup>[11]</sup>

One indication of the importance of leucine-derived compounds is the finding that *M. xanthus* and other myxobacteria exhibit an alternative pathway to IV-CoA, which is also the pre-

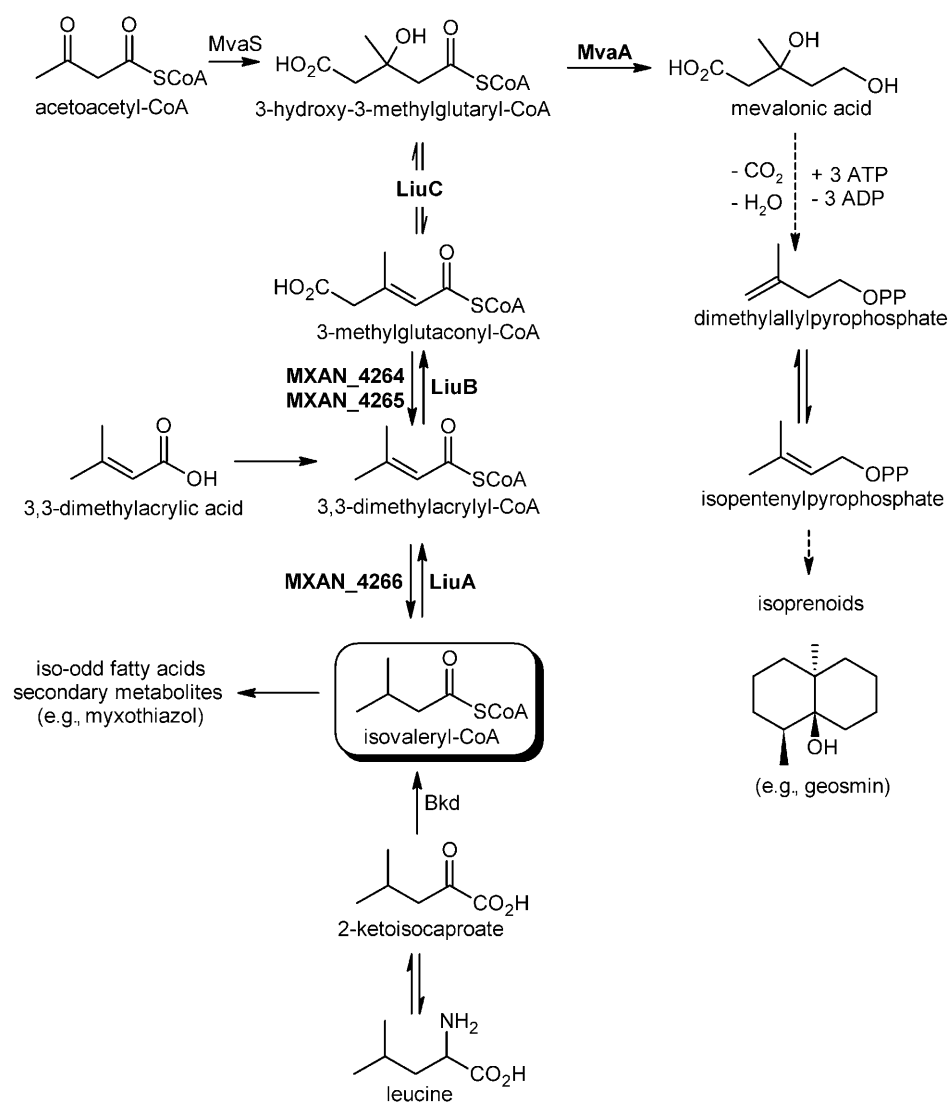
cursor for compounds other than FAs (e.g., myxobacterial secondary metabolites like myxothiazol,<sup>[12]</sup> myxalamids<sup>[13,14]</sup> or aurafurons<sup>[15]</sup>). Feeding experiments in *M. xanthus* and *Stigmatella aurantiaca* led to the prediction of this alternative pathway that branches off the well-known mevalonate-dependent isoprenoid biosynthesis (Scheme 1).<sup>[9,16,17]</sup> This alternative pathway is almost inactive during vegetative growth when leucine is present. However, it is highly induced in *bkd* mutants and during fruiting-body formation when leucine and consequently IV-CoA are limited. We previously confirmed that 3-hydroxy-3-methylglutaryl-CoA (HMG-CoA) synthase (MvaS), which catalyzes the formation of HMG-CoA from acetoacetyl-CoA and acetyl-CoA, is involved in this alternative pathway.<sup>[9]</sup>

Here, we show that *mvaS* is part of a five-gene operon (*aibR*, MXAN\_4264, MXAN\_4265, MXAN\_4266, *mvaS*), the expression of which is up-regulated in *bkd* mutants (Scheme 1). Moreover, the expression of several other genes is altered in *bkd* mutants, which might explain their complex phenotype. The leucine

[a] Dr. H. B. Bode, M. W. Ring, G. Schwär, M. O. Altmeyer, Dr. C. Kegler, Prof. Dr. R. Müller  
Institut für Pharmazeutische Biotechnologie  
Universität des Saarlandes, Postfach 151150  
66041 Saarbrücken (Germany)  
Fax: (+49) 681-3025473  
E-mail: rom@mx.uni-saarland.de

[b] I. R. Jose, Prof. Dr. M. Singer  
Department of Microbiology, One Shields Avenue  
University of California Davis, Davis CA 94616 (USA)

Supporting information for this article is available on the WWW under <http://www.chembiochem.org> or from the author.



**Scheme 1.** Biosynthesis of isovaleryl-CoA and isoprenoids in *M. xanthus* indicating the proposed roles of proteins identified in this study (bold). Dashed arrows indicate multistep reactions.

degradation pathway,<sup>[8]</sup> which is similar to the reverse alternative pathway to IV-CoA, is involved not only in the degradation of IV-CoA, but also in its biosynthesis in *bkd* mutants. Thus, the gene product of MXAN\_3757 (*liuC*) would be predicted to catalyze the dehydration of HMG-CoA to 3-methylglutaryl-CoA (3MG-CoA) and the reverse reaction. Moreover, we show that MXAN\_3759 (*liuB*) and MXAN\_3760 (*liuA*) are indeed involved in the leucine degradation pathway (Scheme 1) but not in the alternative pathway. The missing enzymes for the alternative pathway are most likely encoded in one operon with *mvaS* (MXAN\_4264, MXAN\_4265 and MXAN\_4266) and are predicted to perform the decarboxylation and subsequent oxidation of 3MG-CoA to IV-CoA.

## Results

### Identification of the leucine degradation pathway

The leucine degradation pathway (Scheme 1) has been described in pseudomonads that use acyclic monoterpenes and leucine as their sole carbon sources.<sup>[18–20]</sup> As we speculated that some of the enzymes involved in leucine degradation also act in the alternative biosynthesis pathway to IV-CoA, we aimed to identify the corresponding genes/enzymes from *M. xanthus*. Using LiuC (methylglutaconyl-CoA hydratase) and LiuD (methylcrotonyl-CoA carboxylase) from *Pseudomonas aeruginosa*<sup>[19,20]</sup> as bait we identified the corresponding homologues by BLAST-P searches; all were located together in *M. xanthus*. The product of MXAN\_3757 (renamed *liuC*; leucine and isovalerate utilisation) is a putative methylglutaconyl-CoA hydratase with striking identity/similarity (up to 85%/92%) to several other members of the enoyl-CoA hydratase/isomerase enzyme family (Table 2); MXAN\_3759 (renamed *liuB*) encodes a protein that exhibits high similarity to the  $\alpha$ - and  $\beta$  subunits of propionyl-CoA carboxyltransferase, which can be found in several bacteria.

Thus, we speculate that *liuB* might be involved in the carboxylation of 3,3-dimethylacrylyl-CoA (DMA-CoA) to give rise to 3MG-CoA (Scheme 1). The protein encoded by MXAN\_3760 (renamed *liuA*) shows high homology to short chain acyl-CoA dehydrogenases. The *liuA* gene seems to form an operon with MXAN\_3761–MXAN\_3764, which encode a hypothetical protein, a ribonuclease III and two peptidylprolyl *cis-trans* isomerases, respectively. No function could be assigned to the proteins encoded by MXAN\_3758, MXAN\_3756 and MXAN\_3761 as BLAST-P analysis only revealed similarities to hypothetical proteins from different bacteria (Figure 1, Table 2).

### The leucine degradation pathway is involved in isoprenoid biosynthesis

As leucine was shown to be an efficient precursor for isoprenoids in myxobacteria<sup>[21–23]</sup> we analyzed the incorporation of

**Table 1.** Strains and plasmids used in this study.

Strain or plasmid	Relevant characteristic(s)	Source or reference
<i>E. coli</i>		
DH10B	F <sup>-</sup> <i>mcrA</i> Δ( <i>mrr-hsdRMS-mcrBC</i> ) φ80 <i>lacZ</i> Δ <i>M15</i> Δ <i>lacX74 recA1 endA1 araD139</i> Δ( <i>ara, leu</i> )7697 <i>galU galK</i> λ <sup>-</sup> <i>rpsL</i> ( <i>Str</i> ) <i>nupG</i>	Invitrogen
<i>M. xanthus</i>		
DK1622	wild-type	ref. [44]
DK5643	Δ <i>bkd</i>	ref. [9]
DK5624	Δ <i>bkd, mvaS::kan</i>	ref. [9]
HB001	DK1622::pTOPO3757, <i>Km</i> <sup>r</sup>	this study
HB002	DK5643::pTOPO3757, <i>Km</i> <sup>r</sup>	this study
HB003	DK1622::pTOPO3759, <i>Km</i> <sup>r</sup>	this study
HB004	DK5643::pTOPO3759, <i>Km</i> <sup>r</sup>	this study
HB005	DK1622::pTOPO3760, <i>Km</i> <sup>r</sup>	this study
HB006	DK5643::pTOPO3760, <i>Km</i> <sup>r</sup>	this study
HB011	DK1622::pTOPO4263, <i>Km</i> <sup>r</sup>	this study
HB012	DK5643::pTOPO4263, <i>Km</i> <sup>r</sup>	this study
HB014	DK1622::pTOPO4265, <i>Km</i> <sup>r</sup>	this study
HB015	DK5643::pTOPO4265, <i>Km</i> <sup>r</sup>	this study
HB016	DK1622::pTOPO0082, <i>Km</i> <sup>r</sup>	this study
HB017	DK1622::pTOPO3881, <i>Km</i> <sup>r</sup>	this study
HB018	DK1622::pTOPO5595, <i>Km</i> <sup>r</sup>	this study
HB019	DK5624::pCK4267exp, <i>Km</i> <sup>r</sup> , <i>Zeo</i> <sup>r</sup>	this study
HB020	HB015::pCK4267exp, <i>Km</i> <sup>r</sup> , <i>Zeo</i> <sup>r</sup>	this study
<b>Plasmids</b>		
pCR2.1-TOPO	cloning vector, <i>Km</i> <sup>r</sup>	Invitrogen
pCK_T7A1_att	cloning vector for complementation in <i>M. xanthus</i> , <i>Km</i> <sup>r</sup> , <i>Zeo</i> <sup>r</sup>	this study
pTOPO3757	pCR2.1-TOPO carrying internal fragment of MXAN_3757 ( <i>liuC</i> )	this study
pTOPO3759	pCR2.1-TOPO carrying internal fragment of MXAN_3759 ( <i>liuB</i> )	this study
pTOPO3760	pCR2.1-TOPO carrying internal fragment of MXAN_3760 ( <i>liuA</i> )	this study
pTOPO4263	pCR2.1-TOPO carrying internal fragment of MXAN_4263 ( <i>aibR</i> )	this study
pTOPO4265	pCR2.1-TOPO carrying internal fragment of MXAN_4265	this study
pTOPO0082	pCR2.1-TOPO carrying internal fragment of MXAN_0082	this study
pTOPO3881	pCR2.1-TOPO carrying internal fragment of MXAN_3881	this study
pTOPO5595	pCR2.1-TOPO carrying internal fragment of MXAN_5595	this study
pCK4267exp	pCK_T7A1_att carrying the complete <i>mvaS</i> gene	this study

deuterated leucine (L-5,5,5-[D<sub>3</sub>]leucine) into the sesquiterpene geosmin by feeding the labelled precursor to liquid cultures of DK1622, HB001, HB003 and HB005. Geosmin is one of the major volatile compounds produced by *M. xanthus*<sup>[24]</sup> and was extracted with methanol/*n*-heptane (1:1) from wet cells grown in liquid casitone-tris (CTT) medium. Labelling was determined by GC-MS analysis of the heptane layer according to published procedures. Whereas 5% of total geosmin was D<sub>3</sub>-geosmin in the wild-type cells, no labelling could be observed for any of the mutants; this indicates a complete block in the leucine degradation pathway (Table 3). In order to confirm these results, deuterated 3,3-dimethylacrylic acid (3,3,3,3,3-[D<sub>6</sub>]DMAA) was fed to DK5643, HB002, HB004 and HB006, and geosmin production was analysed. Due to the incorporation of one or

two molecules of DMAA and the loss of one deuterium each during the biosynthesis, 7 and 77% of the expected D<sub>5</sub>- and D<sub>10</sub>-isotopomers<sup>[21]</sup> were observed in DK5643 (Δ*bkd*, Table 3), which is not blocked in the processing of DMAA to geosmin (Scheme 1). Almost identical incorporation rates of 8 and 75% were observed for both geosmin isotopomers in HB006 (Δ*bkd*, MXAN\_3760::*kan*), which when blocked during leucine degradation can be complemented by the addition of DMAA because DMA-CoA is the expected product of isovaleryl-CoA dehydrogenase. No D<sub>5</sub>- or D<sub>10</sub>-geosmin was observed in HB002 (Δ*bkd*, MXAN\_3757::*kan*) or HB004 (Δ*bkd*, MXAN\_3759::*kan*) after feeding of labelled DMAA (Table 3).

In order to identify the biotin carboxylase subunit of the carboxyltransferase MXAN\_3759 we constructed insertion mutants in three (MXAN\_0082, MXAN\_3881 and MXAN\_5595) of the five (MXAN\_1111, MXAN\_5767 also encode such enzymes) biotin carboxylase encoding genes that can be found in the genome of *M. xanthus*. However, analysis of geosmin biosynthesis by feeding of labelled leucine to either mutant resulted in no difference compared to the wild-type cells (data not shown).

#### The leucine degradation pathway is involved in the alternative biosynthesis pathway to isovaleryl-CoA

In order to investigate the influence of the leucine degradation pathway on the biosynthesis of iso-FAs, the FA profiles of DK1622, DK5643 and HB001-HB006 were analysed as described previously.<sup>[9]</sup> No difference in the FA profile of the wild-type cells or mutants in the wild-type background could be observed (data not shown). However, HB002 (Δ*bkd*, *liuC::kan*) showed a decreased amount of iso-FA (Table 4). This finding is similar to the results obtained from a *bkd/mvaS* double mutant described previously.<sup>[9]</sup> The fatty acid profile of HB002 was complemented by the addition of isovalerate (IVA) whereas no difference in the fatty acid profile was observed for the other mutants with or without IVA feeding (data not shown).

#### Comparative proteomics

In order to identify proteins involved in the alternative pathway we performed a differential gel electrophoresis experiment (DIGE) and conventional comparative 2D-gel electrophoresis followed by MALDI-MS analysis of exponentially growing wild-type and *bkd* mutant cells. Although overall 53 proteins could be identified in both experiments (31 were up-regulated and 22 were down-regulated) no candidate proteins that might be involved in the alternative pathway to IV-CoA could be identified (Table S1 in the Supporting Information). However, several ATPase subunits were found to be up-regulated and several regulatory proteins were differentially regulated in *bkd* mutants.

#### Comparative vegetative global gene expression

As proteome analysis did not lead to the identification of putative members of the alternative pathway to IV-CoA, we used a

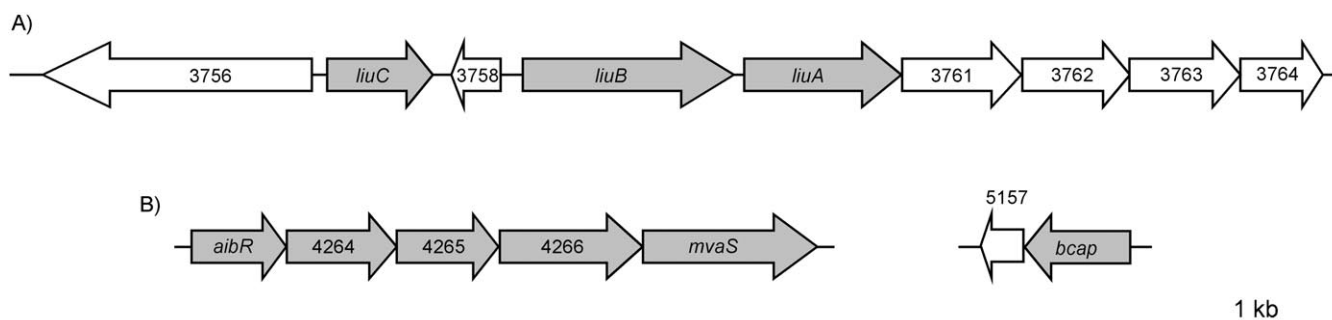


**Figure 1.** Organization of the genomic regions that encode proteins involved in A) the leucine degradation pathway and B) other genes postulated to be involved in the alternative IV-CoA biosynthesis pathway in *Myxococcus xanthus* DK1622. Numbers refer to the *M. xanthus* gene nomenclature (MXAN\_). Genes shown in white are not thought to be involved in IV-CoA formation. For a detailed description of the respective proteins see Table 2 and the text.

Protein	Size [aa]	Deduced function	Protein	Origin	Closest homologue	
					Identities/positives [%]	Accession number
MXAN_3756	654	hypothetical protein	STIAU_6492	<i>Stigmatella aurantiaca</i>	62/74	EAU65620
LiuC	258	3-methylglutaconyl-CoA hydratase	STIAU_6496	<i>S. aurantiaca</i>	85/92	EAU65644
MXAN_3758	119	hypothetical protein	STIAU_6515	<i>S. aurantiaca</i>	66/80	EAU64347
LiuB	513	carboxyl transferase ( $\alpha$ and $\beta$ subunit)	STIAU_6516	<i>S. aurantiaca</i>	86/93	EAU64343
LiuA	381	short chain acyl-CoA dehydrogenase	STIAU_6517	<i>S. aurantiaca</i>	85/95	EAU64345
MXAN_3761	288	hypothetical protein	STIAU_6518	<i>S. aurantiaca</i>	61/63	EAU64351
MXAN_3762	260	ribonuclease III	STIAU_6520	<i>S. aurantiaca</i>	63/80	EAU64340
MXAN_3763	268	peptidylprolyl <i>cis-trans</i> isomerase	STIAU_6521	<i>S. aurantiaca</i>	71/80	EAU64336
MXAN_3764	198	peptidylprolyl <i>cis-trans</i> isomerase	MXAN_1176	<i>M. xanthus</i>	69/82	ABF87515
AibR	228	TetR-like transcriptional regulator	STIAU_3247	<i>S. aurantiaca</i>	76/90	EAU65108
MXAN_4264	265	glutaconate CoA-transferase, subunit A	STIAU_3246	<i>S. aurantiaca</i>	76/84	EAU65098
MXAN_4265	246	glutaconate CoA-transferase, subunit B	STIAU_3245	<i>S. aurantiaca</i>	80/88	EAU65091
MXAN_4266	345	dehydrogenase, Zn binding	STIAU_3244	<i>S. aurantiaca</i>	82/92	EAU65096
MvaS	418	3-hydroxy-3-methylglutaryl-CoA synthase	STIAU_3242	<i>S. aurantiaca</i>	78/88	EAU65112
MXAN_5157	102	hypothetical protein	SACE_2015	<i>Saccharopolyspora erythraea</i>	57/70	CAM01325
Bcap	249	branched-chain amino acid permease	RHA1_ro07263	<i>Rhodococcus</i> sp. RHA1	45/61	ABG99027

Strain	Condition	[D <sub>3</sub> ]Geosmin	[D <sub>5</sub> ]Geosmin	[D <sub>10</sub> ]Geosmin
DK1622	[D <sub>3</sub> ]leucine	5.3	– <sup>[a]</sup>	– <sup>[a]</sup>
	[D <sub>6</sub> ]DMAA	– <sup>[a]</sup>	0.0 <sup>[b]</sup>	0.0 <sup>[b]</sup>
DK5643 ( $\Delta bkd$ )	[D <sub>3</sub> ]leucine	0.0 <sup>[b]</sup>	– <sup>[a]</sup>	– <sup>[a]</sup>
	[D <sub>6</sub> ]DMAA	– <sup>[a]</sup>	7.2	78
HB001 ( <i>liuC</i> )	[D <sub>3</sub> ]leucine	0.0 <sup>[b]</sup>	– <sup>[a]</sup>	– <sup>[a]</sup>
HB002 ( $\Delta bkd$ , <i>liuC</i> )	[D <sub>6</sub> ]DMAA	– <sup>[a]</sup>	0.0 <sup>[b]</sup>	0.0 <sup>[b]</sup>
HB003 ( <i>liuB</i> )	[D <sub>3</sub> ]leucine	0.0 <sup>[b]</sup>	– <sup>[a]</sup>	– <sup>[a]</sup>
HB004 ( $\Delta bkd$ , <i>liuB</i> )	[D <sub>6</sub> ]DMAA	– <sup>[a]</sup>	0.0 <sup>[b]</sup>	0.0 <sup>[b]</sup>
HB005 ( <i>liuA</i> )	[D <sub>3</sub> ]leucine	0.0 <sup>[b]</sup>	– <sup>[a]</sup>	– <sup>[a]</sup>
HB006 ( $\Delta bkd$ , <i>liuA</i> )	[D <sub>6</sub> ]DMAA	– <sup>[a]</sup>	7.6	75

[a] Not expected and not detected; [b] expected but not detected.

global DNA microarray approach to examine vegetative gene expression patterns in *bkd* mutant cells and wild-type cells. As the alternative pathway is highly active in *bkd* cells we expected putative genes involved in this pathway to exhibit significantly higher expression levels in *bkd* cells. As described in the Experimental Section, wild-type and *bkd* mutant cells were

grown to a density of  $5 \times 10^8$  cells mL<sup>-1</sup> (midexponential phase), total cellular RNA was harvested, and the RNA was used for comparative DNA microarray studies. Six independent biological experiments were performed, and based on significance analysis of microarrays (SAM)<sup>[25]</sup> approximately 509 genes were statistically altered in their expression patterns (> or < 2.5-fold) in *bkd* mutant cells compared to wild-type cells. Of these, the largest effect was seen on genes the expression of which was suppressed in the *bkd* mutant strain (471 genes), while 38 genes showed an increase in expression. A partial list of these genes is presented in Table 5 and a complete list of all significantly down- and up-regulated genes (> or < 2.5-fold) is provided in Table S2. The corresponding gene products primarily fall into three groups: 1) hypothetical or conserved hypothetical proteins (~37%); 2) membrane proteins, membrane-associated proteins or proteins involved in membrane/lipid associated processes (25%), and 3) regulatory genes (11%).

The highest up-regulation was observed for MXAN\_4263 (6.1-fold). It shows similarity to TetR-like regulators and was therefore renamed *aibR* (a)lternative i)sovaleryl-CoA b)iosynthesis

**Table 4.** Fatty acid composition [% of total fatty acids] of vegetative cells of *M. xanthus* DK1622 (wild type), DK5643 ( $\Delta bkd$ ), HB002 ( $\Delta bkd$ , *liuC::kan*), HB012 ( $\Delta bkd$ , *aibR::kan*), HB015 ( $\Delta bkd$ , *MXAN\_4265::kan*); both with and without the addition of isovalerate to the growth medium (1 mM); HB19 ( $\Delta bkd$ , *mvaS::kan*, *mvaS<sup>+</sup>*) and HB020 ( $\Delta bkd$ , *MXAN\_4265::kan*, *mvaS<sup>+</sup>*). The two key fatty acids iso-15:0 and 16:1 $\omega$ 5c are shown in bold.

	DK1622	DK5643		HB002		HB012		HB015		HB019	HB020
		–	+IVA	–	+IVA	–	+IVA	–	+IVA		
12:0	0.07	0.04	0.07	0.02				0.11		0.12	
iso-13:0	0.31	0.07	0.41		0.20				0.14	0.19	
iso-14:0		0.22	0.08	0.11	0.02	0.14		0.12		0.16	
14:1 isomer 1	1.41	0.39	1.19	0.14	0.63			0.50	1.05	1.50	0.38
14:1 isomer 2	0.05	0.17	0.12	0.17	0.08	1.05		0.35		0.25	
14:0	5.79	5.36	3.77	4.44	2.22	11.64	5.71	12.13	4.54	9.08	8.13
iso-15:1 $\omega$ 9c	0.32		1.01		0.61	4.54				0.26	
iso-15:1 isomer 2					0.04						
<b>iso-15:0</b>	<b>40.10</b>	<b>19.17</b>	<b>52.16</b>	<b>4.01</b>	<b>47.76</b>	<b>3.81</b>	<b>58.85</b>	<b>2.70</b>	<b>56.87</b>	<b>41.37</b>	<b>3.47</b>
15:0	1.75	8.46	1.93	18.06	1.54	56.87		12.15	0.82	2.15	14.07
15:1 isomer 1	2.43	3.06	1.17	3.91	1.23	0.82		3.24	2.05	1.37	5.22
15:1 isomer 2	3.35	0.21	2.06	0.21	2.09	2.05		4.43	1.22	1.47	4.33
iso-16:0	0.01	7.17	1.42	7.11	0.63	1.22		2.67	0.19	1.93	2.51
16:2 $\omega$ 5c,11c	5.46	3.77	5.10	2.74	4.24	0.19	5.20	4.00	6.07	5.49	4.28
16:1 $\omega$ 11c	0.90	1.48	0.51	1.58	0.49	6.07		2.44		1.10	2.97
<b>16:1<math>\omega</math>5c</b>	<b>17.04</b>	<b>29.14</b>	<b>10.92</b>	<b>37.93</b>	<b>10.87</b>	<b>41.01</b>	<b>17.10</b>	<b>38.23</b>	<b>13.24</b>	<b>15.83</b>	<b>36.18</b>
16:0	1.58	5.88	1.85	7.04	1.44	13.24	3.27	11.32	1.41	3.64	12.31
iso-17:2 $\omega$ 5c,11c	1.93	0.28	1.97	0.04	2.68	1.41			1.28	1.37	
iso-17:1 $\omega$ 11c	0.69	0.27	0.55		0.76	1.28			0.49	0.66	
iso-17:1 $\omega$ 5c	1.73	1.04	1.98	0.18	3.38	0.49			1.14	1.34	
iso-17:0	2.89	4.66	2.82	1.46	4.88	1.14	4.80	0.31	3.48	4.71	0.71
14:0 3-OH	0.45	1.43	0.35	5.96	0.35	3.48	0.32	2.11	0.26	0.59	1.53
iso-15:0 3-OH	2.15	1.32	1.85	0.34	2.78	0.26	1.42	0.14	1.82	1.94	0.22
16:0 2-OH	0.35	1.02	0.28	1.74	0.29	1.82	0.14	0.94	0.11	0.08	1.58
16:0 3-OH	0.38	0.37	0.33	0.90	0.14	0.11		1.88	0.11	0.39	1.53
iso-17:0 2-OH	4.10	3.90	3.28	1.51	6.57	0.11	2.96	0.21	2.95	1.42	0.46
iso-17:0 3-OH	1.82	0.38	0.25	0.33	0.53	2.95	0.24	0.03	0.23	0.76	0.10
iso-15:0 DMA <sup>[a]</sup>	2.19	0.51	2.06		2.60	0.23			0.49	0.59	
iso-15:0 OAG <sup>[b]</sup>	0.74	0.22	0.49	0.08	0.94	0.49				0.25	

[a] Dimethylacetal; [b] 1-O-alkylglycerol.

regulator), which is the first gene within a five-gene operon (Figure 1) that includes *mvaS* (MXAN\_4267; 2.62-fold up-regulated). The *mvaS* gene was already shown to be up-regulated in a *bkd* mutant.<sup>[9]</sup> However, in an early draft version of the *M. xanthus* genome<sup>[26]</sup> *mvaS* was located on a different stretch of contiguous DNA and thus no operon structure could be deduced for *mvaS* and its neighbouring genes in previous work. Other genes in this operon are MXAN\_4264 and MXAN\_4265 which show similarity to the two subunits of glutaconyl-CoA transferases. Additionally, MXAN\_4266, which encodes a protein that is similar to Zn-dependent dehydrogenases, was identified in the operon and was found to be up-regulated by 2.73-fold.

The only other gene that might be involved in the alternative pathway due to its predicted enzymatic function was MXAN\_5158 renamed *bcap* as it encodes a putative branched-chain amino acid permease that forms an operon with a gene that encodes a hypothetical protein (Figure 1, Tables 2 and 5). Additionally, several sequences encoding regulatory genes and transporters as well as hypothetical proteins were up-regulated (Table 5). The majority of genes that were down-regulated encode hypothetical or regulatory proteins (Tables 5 and S2).

Additionally, several genes encoding proteins involved in lipopolysaccharide (MXAN\_6398, MXAN\_4726, MXAN\_1639) or sugar biosynthesis (MXAN\_6497) were found to be down-regulated.

In order to confirm the microarray data we performed quantitative reverse transcript PCR (qRT-PCR) analysis of selected genes as described previously.<sup>[9]</sup> As expected, *aibR*, MXAN\_4264, MXAN\_4265 and MXAN\_4266 showed a similar transcription profile as described for *mvaS*.<sup>[9]</sup> Overall, the high level of transcripts in the *bkd* mutant was decreased to wild-type levels by the addition of IVA (Figure 2A–D). No such results could be obtained for *bcap*, *liuC* and *liuA*, which were also analyzed (Figure 2E–G). We also analyzed the expression of MXAN\_5020 (*mvaA*) and MXAN\_5021, which encode the HMG-CoA reductase and isopentenylidiphosphate isomerase, respectively. Both enzymes are involved in the transformation of HMG-CoA to isopentenylidiphosphate and dimethylallyldiphosphate, respectively, which are the universal building blocks of the isoprenoids. However, no difference between the expression of the latter two genes was observed between the wild-type and *bkd* mutant cells with or without the addition of IVA (Figure 2H, *mvaA*, and data not shown, MXAN\_5021).

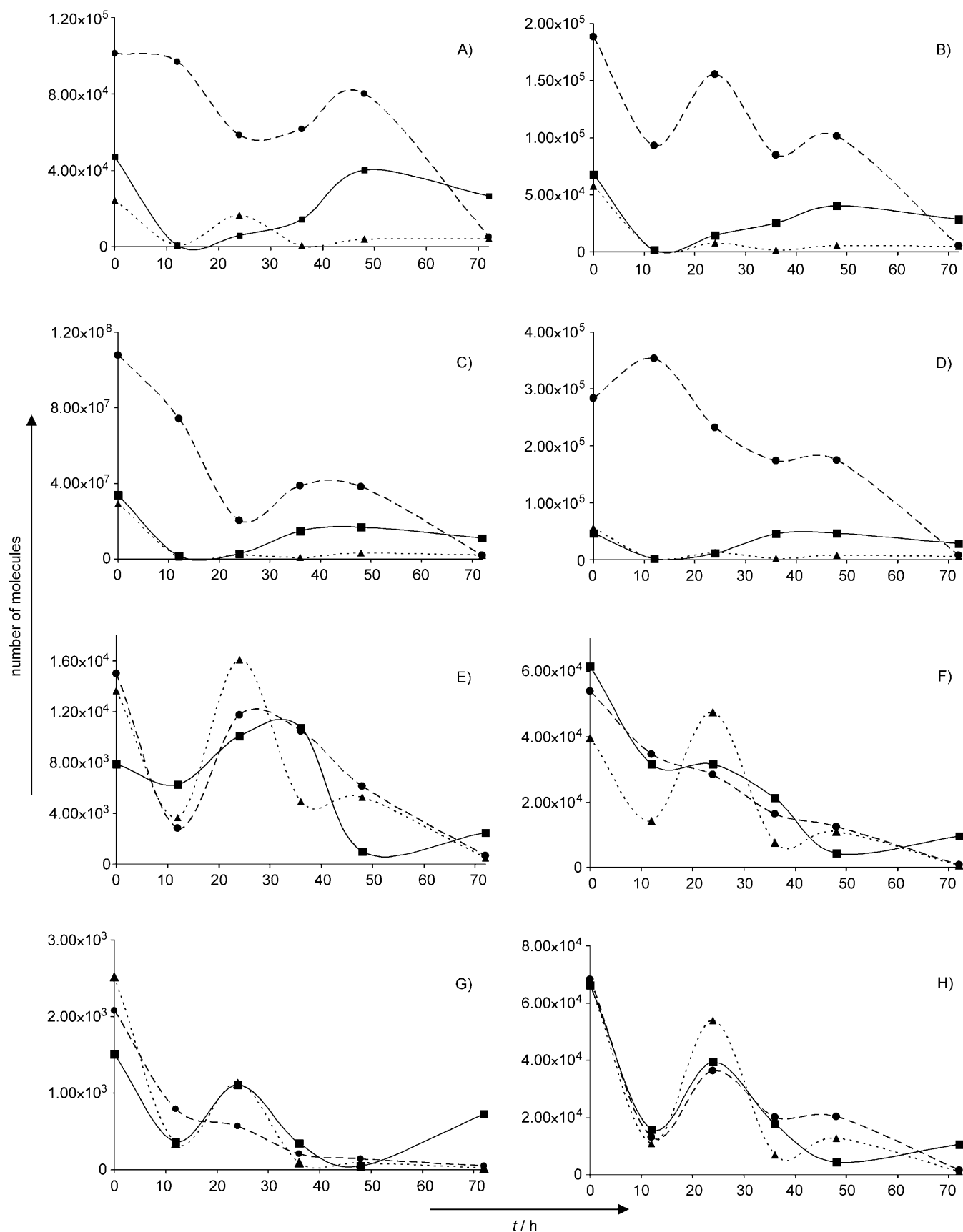


**Figure 2.** Transcript numbers for selected genes during vegetative growth of DK1622 (■), DK5643 (●), DK5643 + 1 mM IVA (▲). A) *AibR*, B) *MXAN\_4264*, C) *MXAN\_4265*, D) *MXAN\_4266*, E) *liuC*, F) *liuA*, G) *bcap* and H) *mvaA*. For *mvaS* transcript numbers and growth curves of the different strains see ref. [9]. Mean values of two or three independent experiments are shown.

### Functional analysis of genes found up-regulated in the *bkd* mutant

Plasmid insertions into *aibR* and MXAN\_4265 in a wild-type background resulted in no change of phenotype with respect to fatty acid and/or geosmin biosynthesis (data not shown) as also described for a *mvaS* mutant. However, in a  $\Delta bkd$  background both double mutants showed the phenotype of a *bkd/mvaS* strain, which is characterized by a very low amount of iso-FAs (Table 4) and the production of only trace amounts of geosmin (Table 3). This phenotype could be complemented to wild-type levels by the addition of IVA or DMAA.

However, as an insertion into any gene of the *aibR-mvaS* operon would most likely exhibit polar effects and thus directly influence expression of *mvaS*, we complemented the  $\Delta bkd/mvaS$  (DK5624) and  $\Delta bkd/MXAN_4265$  (HB015) double mutants genetically by addition of a copy of *mvaS* under control of the constitutive T7A1-promotor,<sup>[27]</sup> this resulted in strains HB019 ( $\Delta bkd, mvaS::kan, mvaS^+$ ) and HB020 ( $\Delta bkd, MXAN_4265::kan, mvaS^+$ ). Whereas the fatty acid profile of HB019 was similar to the wild-type cells as expected, no complementation was observed for HB020 (Table 4).

Despite several attempts, we were not able to generate a *bcap* mutant by plasmid insertion.

## Discussion

### The leucine degradation pathway is involved in the alternative pathway to IV-CoA

Plasmid insertion into genes of *M. xanthus* that have been identified by homology searches by using genes from different *Pseudomonas* strains<sup>[19,20]</sup> confirmed the involvement of several genes in the degradation of leucine also in the alternative pathway to IV-CoA. Mutants of *liuA-C* still produce isoprenoids, like geosmin, but do not perform leucine-dependent isoprenoid biosynthesis (Table 3). Leucine is a major amino acid constituent of bacteria, which are a major food source for *M. xanthus*. Therefore, leucine also seems to be a major source for isoprenoids via the leucine degradation pathway that enters the mevalonate dependent isoprenoid biosynthesis via HMG-CoA.<sup>[8]</sup> A *bkd/liuC* double mutant shows a similar phenotype to a *bkd/mvaS* mutant strain, which produces only residual amounts of iso-FAs. The remaining trace amounts of iso-FAs might be derived from a second *bkd* activity.<sup>[7]</sup> This indicates that the *liuC*-encoded methylglutaconyl-CoA hydratase catalyses the hydration of 3-methylglutaconyl-CoA to HMG-CoA and its reverse dehydration. No reduction in the amount of iso-FAs was observed for *bkd/liuB* or *bkd/liuA* double mutants. The *LiuB* protein shows similarity to the  $\alpha$ - and  $\beta$  subunits (the carboxyltransferase subunits) of a biotin dependent carboxylase, and therefore might well be involved in the carboxylation of dimethylacryloyl-CoA, whereas the decarboxylation might be catalyzed by a different enzyme (see below). *LiuA* shows similarities to acyl-CoA dehydrogenases, and might be involved in the oxidation of IV-CoA to DMA-CoA and the reverse reduction. However, at least eleven similar dehydrogenase-encoding

genes are present in the genome<sup>[28]</sup> which might complement a *liuA* mutant. Interestingly, this does not seem to occur in the oxidative reaction as a *liuA* mutant shows no geosmin production from leucine. However, a *bkd/liuA* mutant shows the production of geosmin from labelled DMAA as this complements the *liuA* block of the pathway (Table 3). Alternatively, MXAN\_4266 might catalyze the reduction of DMA-CoA to IV-CoA (see below).

The fact that the expression of genes involved in leucine degradation/IV-CoA biosynthesis is not increased in *bkd* mutants might indicate that the expression is already maximal (due to the effective use of leucine as carbon source) or that translational regulation occurs.

We also tried to identify the biotin carboxylase partner of the *LiuB* carboxyltransferase. However, disruption of three possible candidates, MXAN\_0082, MXAN\_3881 and MXAN\_5595, did not result in a difference compared to the wild-type cells with respect to fatty acid or geosmin biosynthesis (data not shown). This might indicate that either one of two remaining genes that encode such enzymes, MXAN\_1111 or MXAN\_5767, might be the missing subunit or that these enzymes can functionally complement each other, which seems to be more likely. Interestingly, *LiuB* is the only "orphan" carboxylase subunit as all other carboxylase subunit encoding genes are found associated with other carboxylase subunits (data not shown).

### Comparative global expression confirmed the complex phenotype of the *bkd* mutant

Comparative proteome analysis between wild-type and *bkd* mutant cells led to the identification of several changes in the proteome of the *bkd* mutant (Table S1) but did not lead to identification of enzymes putatively involved in the alternative pathway to IV-CoA. Luckily, comparison of global expression pattern between wild-type and *bkd* cells under vegetative conditions was much more successful and led to the identification of a five-gene operon, which was highly expressed in *bkd* cells (Table 5, Figure 2). Interestingly, only little direct overlap (MXAN\_0433, MXAN\_0709—both hypothetical proteins—and MXAN\_1450—OmpA-related protein) could be observed between the proteome and transcriptome data. This can be due to a much smaller number of protein spots that have been analyzed compared to an almost complete list of genes. The fact that less abundant proteins are much more difficult to detect compared to less abundant transcripts might be another reason for this discrepancy. Additionally, from the way the proteome comparisons were made, a difference between no protein at all (sample 1) and small amounts of protein (sample 2) would only be detected in a DIGE experiment but not in the standard Coomassie experiment with the software used (see the Experimental Section).

### The missing genes of the alternative pathway to IV-CoA are encoded in one operon with *mvaS*

From the transcriptome analysis the *aibR-mvaS* operon was identified, in which *mvaS*, which encodes the HMG-CoA syn-

these, was already identified as being part of the alternative pathway.<sup>[9]</sup> From the other proteins encoded in this operon AibR shows similarity to TetR-like regulators, MXAN\_4264 and MXAN\_4265 encode two subunits of a glutaconyl-CoA transferase and MXAN\_4266 encodes a dehydrogenase. Glutaconyl-CoA transferases are involved in fermentative glutamate degradation and catalyze the transfer of a CoA moiety from acetyl-CoA to glutaconate, a glutamate degradation product.<sup>[29]</sup> The resulting glutaconyl-CoA is then decarboxylated to crotonyl-CoA, which is subsequently converted to two acetyl-CoA units as shown in *Acidaminococcus fermentans*.<sup>[30,31]</sup> The glutaconyl-CoA decarboxylase involved in this process was shown to be a membrane bound sodium pump that consists of four subunits of which no homologues can be found in *M. xanthus*, except for the carboxylase  $\alpha$  subunit, which shows highest identity/similarity to LiuB (27%/49%) but also to AccB (acetyl-CoA carboxylase, 24%/43%) and PccB (propionyl-CoA carboxylase, 24%/41%). Although glutaconyl-CoA and 3-methylglutaconyl-CoA—believed to be an intermediate in the alternative pathway to IV-CoA—differ only in one methyl group, all intermediates in the alternative pathway seem to be CoA-bound and thus no activation of a free acid seems to be required. Moreover, MXAN\_4264, MXAN\_4265 and MXAN\_4266 are not involved in the leucine-dependent isoprenoid biosynthesis as a *bkd/aibR* mutant, which produces only trace amounts of geosmin, can be complemented by the addition of DMAA (Table 3). Moreover, an involvement of glutaconyl-CoA in the conversion of mevalonate to 3MG-CoA in a mevalonate shunt pathway, which was proposed more than 30 years ago,<sup>[32]</sup> can be excluded as we performed feeding experiments with [1,2-<sup>13</sup>C<sub>2</sub>]mevalonolactone in DK1622 and DK5643, but could not see any incorporation of label into iso-FAs (data not shown). Similar results were observed earlier from feeding experiments in *bkd* mutants of *S. aurantiaca* Sg a15 which clearly incorporates labelled mevalonolactone (the lactone form of mevalonate) into isoprenoids like aurachin but not into isovaleryl-CoA derived compounds like myxothiazol.<sup>[17]</sup>

In order to elucidate the importance of MXAN\_4264, MXAN\_4265 and MXAN\_4266 with respect to the alternative pathway, we genetically complemented strain HB015 ( $\Delta bkd$ /MXAN\_4265) and as a control DK5624 ( $\Delta bkd/mvaS$ ) with an intact copy of *mvaS*. No complementation of the fatty acid profile was observed for HB020 ( $\Delta bkd$ , MXAN\_4265::*kan*, *mvaS*<sup>+</sup>) whereas wild-type levels of iso-FAs were detected in HB019 ( $\Delta bkd$ , *mvaS*::*kan*, *mvaS*<sup>+</sup>). This clearly demonstrates a function of at least MXAN\_4265 or MXAN\_4266 in the transformation of 3-methylglutaconyl-CoA to isovaleryl-CoA. Our current hypothesis is, that MXAN\_4264 and MXAN\_4265 are involved in the decarboxylation of 3-methylglutaconyl-CoA to 3,3-dimethylacrylyl-CoA, and MXAN\_4266 is involved in the final reduction to IV-CoA. While the latter reaction sounds reasonable for the encoded enzyme, no decarboxylase function has to our knowledge been assigned to enzymes that show homology to CoA transferases in the literature. Currently MXAN\_4264, MXAN\_4265 and MXAN\_4266 are expressed in order to evaluate this hypothesis in in vitro experiments that employ recombinant enzymes.

Database analysis of the *aibR-mvaS* operon revealed that it is identical to an operon studied by the Kroos group several years ago.<sup>[33]</sup> However, at the time of their work, no information about the fifth gene in the operon (*mvaS*) was available due to the small contig size in the draft genome sequence,<sup>[26]</sup> as already mentioned. Their aim was to characterize the  $\Omega$ 4514 regulatory region. The  $\Omega$ 4514 region is the site of a Tn5 *lac* insertion in the *M. xanthus* genome that does not depend on C signalling for expression and yet is expressed with a timing during development similar to that of promoters that depend on C signalling. The C signal is the best characterized signal required for fruiting-body formation in *M. xanthus*.<sup>[34]</sup> It is a protein encoded by the *csgA* gene, which is involved in aggregation and finally also sporulation during development of *M. xanthus*. The current hypothesis suggests that the CsgA protein is transferred between cells in a cell-cell contact dependent manner and it is involved in the expression of several other developmental genes.<sup>[35]</sup> The  $\Omega$ 4514 Tn5 *lac* is inserted in the third codon of MXAN\_4265 and Kroos and colleagues could show that expression is strongly induced during development. This fits well to our previous experiments that show that the activity of the alternative pathway to IV-CoA can also be detected during development in the wild-type.<sup>[9]</sup> Moreover, they could show that MXAN\_4263 (*aibR*) negatively regulates the whole operon, but did not detect direct binding of MXAN\_4263 to the promoter region. They speculated that this might be due to additional low-molecular weight factors that are missing in the in vitro binding assay similar to the case of tryptophan and the *trp* repressor.<sup>[36]</sup> In fact, given the current knowledge one can speculate even more, that IV-CoA or one of the pathway intermediates that lead to IV-CoA might be such a factor. In order to learn more about the function of this operon, in vitro studies of the purified proteins are in progress to identify their substrates and regulation.

The gene MXAN\_5158 (*bcap*) encoding a branched chain amino acid transporter was also highly expressed in the *bkd* mutant. Surprisingly, no mutants in *bcap* could be obtained in the wild-type or *bkd* mutant cells by plasmid insertions despite several attempts. This is surprising as we have usually had no problems in the generation of mutants using this approach. This might suggest that *bcap* is essential as it might be an important leucine transporter in *M. xanthus*, although several other transporters (most with unknown substrate specificity) can be found in the genome (data not shown).

Mutants in the *bkd* genes have a complex phenotype; they show not only a reduction in the amount of iso-FAs to half of the amount of the wild-type cells,<sup>[5,7]</sup> but they are also delayed in aggregation, produce less myxospores<sup>[7,10]</sup> and can hardly develop in submerge culture. For the latter it is crucial that the cells settle at the bottom of a microtiter plate or Petri dish. Whereas the wild-type forms a tightly bound layer of cells at the bottom of the well, the cell layer of a *bkd* mutant is very loose and cells brake away from the bottom very easily (unpublished observations). The reason for this might be a change in the exopolysaccharide/fibril (or slime) composition or in the composition of the outer membrane. Therefore, it is not surprising that the expression of genes involved in lipid or

membrane biosynthesis like MXAN\_6398, MXAN\_4726 and MXAN\_1639 (Table 5) is down regulated in a *bkd* mutant. The observed down regulation of lipoproteins like MXAN\_2391, MXAN\_5414 or MXAN\_4653 might also be involved in the non-adhesive phenotype of the *bkd* mutant.

In order to correlate these data to the *bkd* phenotype, we compared wild-type and *bkd* mutant cells in a Trypan blue assay that measures fibril polysaccharide content.<sup>[37]</sup> In accordance with the nonadhesive phenotype and the down-regulated genes in the *bkd* mutant, only half (4.4%) the level of Trypan blue binding could be identified compared to the wild-type cells (8.7%); this indicates that only half the amount of fibril material is present in the mutants.

Interestingly, many more genes could be identified the expression levels of which were down- rather than up-regulated. Moreover, many of the down-regulated genes encode various forms of regulatory proteins that might be involved in the complex phenotype of the *bkd* mutant.

As *M. xanthus* contains 18 gene clusters for the biosynthesis of secondary metabolites<sup>[28,38]</sup> it is not too surprising that several of them are influenced in the *bkd* mutant: expression of MXAN\_4601, MXAN\_3619 and *taP* (MXAN\_3932) is strongly reduced in a *bkd* mutant. In almost all secondary-metabolite producing organisms many more biosynthesis gene clusters than secondary metabolites can be identified,<sup>[39]</sup> and the biosynthesis gene clusters that cannot be correlated to actual compounds are usually called "silent". However, the identification of MXAN\_4601 and MXAN\_3619 proves that the corresponding biosynthesis gene clusters are not silent but are expressed in wild-type cells as is also the case for *taP*, which is involved in myxovirescin biosynthesis.<sup>[40]</sup> The reason why no secondary metabolite has been identified for these two biosynthesis gene clusters might simply be a very low production of the corresponding compound just to name one possible reason. With respect to secondary metabolism, one can conclude from these data that actually 12 of the 18 biosynthesis gene clusters are expressed in the wild-type cells during vegetative growth; this is in fact a very high number. Five secondary metabolites have already been isolated and correlated to the respective biosynthesis gene clusters<sup>[14,40–42]</sup> and the expression of five additional biosynthesis gene clusters have been shown by analysis of the proteome.<sup>[43]</sup>

In summary, we could identify the leucine degradation pathway in *M. xanthus*, which also serves as anabolic pathway to isoprenoids and is involved in the alternative pathway to IV-CoA. Moreover, global expression analysis of a *bkd* mutant and wild-type cells resulted in the identification of an operon that harbours a set of genes (*aibR*, MXAN\_4264, MXAN\_4265, MXAN\_4266, *mvaS*) that are most likely all involved in the alternative IV-CoA biosynthesis pathway. Furthermore, several additional genes have been identified that are either up- or down-regulated, and reveal a complex regulatory network that is changed in the *bkd* mutant. In vitro work is currently in progress to biochemically characterise the proteins encoded by the genes in the operon(s) identified in this study.

Moreover, our data offer a link between the myxobacterial "lifestyle", leucine biosynthesis and the alternative pathway to

IV-CoA. It has been a puzzle for a long time why *M. xanthus* fails to synthesize leucine as one of the most common amino acids although its large genome would easily have the capacity for leucine biosynthesis. A possible explanation for the predatory lifestyle of *M. xanthus* would be that prey are a convenient source of leucine. However, it would be very inefficient to degrade all the available prey leucine to IV-CoA, which is required for iso-FA synthesis. The more efficient solution might be to use leucine directly for protein biosynthesis and to supplement the pathway to IV-CoA and subsequently iso-FAs and secondary metabolites with endogenous pathways. Similarly, leucine degradation to IV-CoA during starvation conditions (leucine depletion) seems to be very risky as large amounts of leucine is required for protein synthesis to complete myxobacterial development. This theory would help to explain why the alternative pathway to IV-CoA is up-regulated during myxobacterial development.

## Experimental Section

**Strains, culture conditions, mutant construction and complementation strategy:** *Myxococcus xanthus* DK1622 (wild type)<sup>[44]</sup> and all of its descendants were routinely grown in CTT medium<sup>[45]</sup> with kanamycin (40 µg mL<sup>-1</sup>) where appropriate. Feeding experiments with [D<sub>3</sub>]leucine and [D<sub>6</sub>]DMAA have been described previously.<sup>[9,17,21]</sup> For the construction of mutants, internal fragments (~600 bp) of MXAN\_3757, MXAN\_3759, MXAN\_3760, MXAN\_4263, MXAN\_4265, MXAN\_5158, MXAN\_0082, MXAN\_3881 and MXAN\_5595, were amplified by PCR from genomic DNA of DK1622 by using the oligonucleotides 3757-1 (5'-CCGGAATCAAGGTCGACGC-3'), 3757-2 (5'-AAGGCCTCTGCGCGTTGAT-3'), 3759-1 (5'-TTCGTG-GAGGACGCGAAGCT-3'), 3759-2 (5'-TCTCCACCTTCTTGCCGC-3'), 3760-1 (5'-AAGCCGATGCCCCGTGAGTG-3'), 3760-2 (5'-TCCACGTTCCAGGACGAG-3'), 4263-1 (5'-ACGAACACCGGAGGACGGAA-3'), 4263-2 (5'-CGTGCTCTGGAGGATGATG-3'), 4265-1 (5'-TGGACATCA-CCCCAGCGGAGA-3'), 4265-2b (5'-AACTTCGTCGCGGCTTGCC-3'), 5158-1 (5'-ATGGGGCATGTGGATCGAAG-3'), 5158-2 (5'-GAACGCCACGGACTCGTCCA-3'), 06613-1 (5'-TGGCCATTGGTCCGTCTC-3'), 06613-2 (5'-GGTAGCCAATCGCCGAG-3'), 02236-1 (5'-ATCACCTGGAG-GGCGAC-3'), 02236-2 (5'-TCCTCTGCCGGGAGATG-3'), 5595-1 (5'-ACGGTCGCGCTATTTCGGA-3') and 5595-2 (5'-GGAACATCCCGCTC-CAGAC-3'), respectively. The resulting fragments were cloned into pCR2.1-TOPO (Invitrogen) to give plasmids pTOPO3757, pTOPO3759, pTOPO3760, pTOPO4263, pTOPO4265, pTOPO5158, pTOPO0082, pTOPO3881 and pTOPO5595, which were introduced into *M. xanthus* DK1622 or DK5643 (*Δbkd*)<sup>[9]</sup> by electroporation as described previously.<sup>[14,46]</sup> This resulted in strains HB001–HB006, HB011, HB012, HB014–HB018 (Table 1). The correct integration of each plasmid was confirmed for all strains by using a PCR protocol based on a plasmid- and gene-specific primer pair as described previously.<sup>[46]</sup>

For construction of an *mvaS* expression plasmid a 1.3 kbp fragment containing the MXAN\_4267 (*mvaS*) gene was amplified from genomic DNA of *M. xanthus* DK1622 by using oligonucleotides 4267exp\_HindIII/NdeI-1 (5'-ATATAAGCTTGCATATGAAGAAGCGCGTG-GGAATC-3') and 4267exp\_XhoI-2 (5'-ATATCTCGAGGTCAGTTC-CCTTCGGCGTAC-3'). This product, which contained the gene with an NdeI restriction site (underlined) at its start codon (in bold), was digested with HindIII and XhoI (restriction sites underlined) and cloned into pBluescript SK(+) (Stratagene). The gene was isolated from the resulting plasmid with NdeI and XhoI and cloned into

**Table 5.** Genes showing changes in expression by DNA microarray analysis comparing DK5643 (*Δbkd*) with DK1622 (wild type). Up- and down-regulation refers to the *bkd* mutant. Genes in bold are discussed in the text.

MXAN#	TIGR annotation	x-fold up	MXAN#	TIGR annotation	x-fold down
MXAN_4263	transcriptional regulator, TetR family	6.10	MXAN_7208	serine/threonine protein kinase	10.42
MXAN_2957	RNA polymerase sigma-D factor, authentic frame-shift	4.87	MXAN_1185	sulfatase family protein	10.39
<b>MXAN_5158</b>	AzIC family protein	4.12	MXAN_6797	putative membrane protein	10.22
MXAN_6934	ABC transporter, ATP-binding/permease protein	3.86	MXAN_2931	lipoprotein, putative	10.21
MXAN_3862	Na <sup>+</sup> /H <sup>+</sup> ion antiporter	3.60	MXAN_5666	ATPase, AAA family	10.09
MXAN_0352	ribosomal protein S6 modification protein	3.50	MXAN_6621	glycosyl hydrolase, family 3	9.81
MXAN_4173	ABC transporter, permease protein, putative	3.19	MXAN_5414	lipoprotein, putative	9.79
MXAN_4977	sigma-54 dependent DNA-binding response regulator	3.01	MXAN_0369	signal peptidase II	9.62
MXAN_1450	ompa-related protein precursor	2.99	MXAN_3694	glycosyl hydrolase, family 13	9.55
MXAN_3644	isochorismatase	2.90	MXAN_5205	methylated-DNA-[protein]-cysteine S-methyltransferase family protein	9.49
MXAN_3711	DNA-binding response regulator, LuxR family	2.84	MXAN_0980	cytochrome c family protein	9.48
MXAN_6646	transcriptional regulator, MarR family	2.82	MXAN_2116	sensor histidine kinase, authentic frame-shift	9.42
MXAN_4445	sensory box histidine kinase/response regulator	2.79	MXAN_2230	transcriptional regulator, LuxR family	9.36
MXAN_3958	tRNA pseudouridine synthase D	2.78	MXAN_2775	PDZ domain protein	9.32
MXAN_6199	putative proline racemase	2.77	MXAN_6664	branched-chain amino acid ABC transporter, permease protein LivH	9.26
<b>MXAN_4266</b>	oxidoreductase, zinc-binding dehydrogenase family	2.73	MXAN_6579	TonB-dependent receptor, putative	9.25
<b>MXAN_4267</b>	HMG-CoA synthase	2.62	MXAN_4676	peptidylprolyl <i>cis-trans</i> isomerase, cyclophilin-type	9.16
MXAN_6514	undecaprenol kinase, putative	2.72	MXAN_0006	peptidase, M16 (pitrilysin) family, authentic frame-shift	9.15
MXAN_0976	lipoprotein, putative	2.57	MXAN_7044	BNR/Asp-box repeat domain protein	8.91
MXAN_1530	HAD-superfamily subfamily IB hydrolase, TIGR01490	2.51	MXAN_3868	cytochrome c oxidase, subunit I	8.89
MXAN_6223	sensor histidine kinase	21.08	MXAN_3292	putative chaperone protein DnaJ	8.82
MXAN_6415	ompa-related protein precursor	16.06	MXAN_0335	5-3 exonuclease family protein	8.77
MXAN_2391	lipoprotein, putative	15.49	MXAN_4576	acetyltransferase, GNAT family	8.75
MXAN_2323	outer membrane protein, OMP85 family	14.05	MXAN_5562	cytochrome c peroxidase	8.67
MXAN_5098	putative Ig domain protein	13.57	MXAN_6924	SPFH/band 7 domain protein	8.63
<b>MXAN_6398</b>	3-oxoacyl-acyl carrier protein reductase, putative	13.38	MXAN_0432	metallo-β-lactamase family protein	8.59
<b>MXAN_4726</b>	UDP-3-O-[3-hydroxymyristoyl]glucosamine N-acyltransferase	13.36	MXAN_2079	adenylosuccinate lyase	8.59
<b>MXAN_1639</b>	CDP-tyvelose-2-epimerase	12.75	MXAN_2429	ABC transporter, permease protein	8.59
MXAN_3734	response regulator	12.53	MXAN_7310	oxidoreductase, short chain dehydrogenase/reductase family	8.56
MXAN_6750	transcriptional regulator, LuxR family	12.50	MXAN_2015	ATP-dependent Clp protease, ATP-binding subunit ClpX	8.28
MXAN_2282	oxidoreductase, zinc-binding dehydrogenase family	11.78	MXAN_5348	M23 peptidase domain protein	8.05
MXAN_4003	oxidoreductase, aldo/keto reductase family	11.19	MXAN_3153	ethanolamine ammonia lyase, large subunit/small subunit	8.02
MXAN_4712	glycosyl transferase, group 1 family protein	11.19	MXAN_6497	glucokinase	7.95
MXAN_2524	homoserine kinase, putative	11.12	MXAN_4653	lipoprotein, putative	7.87
MXAN_7414	molybdopterin-guanine dinucleotide biosynthesis protein B/formate dehydrogenase family accessory protein FdhD	10.90	MXAN_0258	ATPase domain protein	7.76
MXAN_3386	aspartate aminotransferase, putative	10.71	MXAN_6843	putative membrane protein	7.63
MXAN_3903	efflux transporter, AcrB/AcrD/AcrF family, inner membrane component	10.68	MXAN_1668	serine/threonine kinase associate protein KapC	7.41
MXAN_0325	membrane protein, putative	10.63	MXAN_3320	adenylate kinase	7.38
MXAN_0614	serine/threonine protein kinase	10.53	MXAN_5781	efflux ABC transporter, ATP-binding protein PilH	7.10
MXAN_5558	cytochrome c, putative	10.44	<b>MXAN_4601</b>	nonribosomal peptide synthase	7.09

pCK\_T7A1\_att. For the construction of pCK\_T7A1\_att a pCR2.1-TOPO vector containing an insert was digested with EcoRI and religated to create pCR2.1\_EcoRI, which had a single EcoRI restriction site. For insertion of a terminator the annealed oligonucleotides ter\_dw (5'-GGCCAAAAGGATCTTCACCTAGATCCTTTTCTAGAT-

GCA-3') and ter\_up (5'-TCTAGAAAAGGATCTAGGTGAAGATCCTTTT-3') were ligated into the Mph1103I/Bsp120I digested pCR2.1\_EcoRI vector to give pTOPO\_ter. The zeocin resistance gene and its promoter was PCR amplified from the vector pPICZ B (Invitrogen) by using the primers ET\_zeo\_box\_1 (5'-CTGGCGCCGTTACTAGT-

GGATCCGAGCTCGGTACCAAGCTTGGCGTAATGGATCTGATCAGCACG-TGTTGACA-3') and ET\_zeo\_box\_2 (5'-TCGCCGAGCCGAACGACC-GAGCGCAGCGAGTCAGTGAGCGAGGAAGCGGTGATCACACGTGTCA-GTCCTGCTCCTCGGCCACG-3') to give a 570 bp fragment, which was subsequently cloned into pTOPO\_ter by standard ET-cloning procedures.<sup>[47–49]</sup> The *lacZ* promoter region was deleted at the same time to give pTOPO\_zeo\_core. This plasmid was digested with BamHI/HindIII, and the T7AI promoter sequence was inserted through the annealed oligonucleotides T7A1\_up (5'-AGCTTAT-CAAAAAGAGTATTGACTTAAAGTCTAACCTATAGGATACTTACAGCCAT-CGAGAGGTGTACATATGG-3') and T7A1\_dw (5'-GATCCCATATGTACA-CCTCTCGATGGCTGTAAGTATCTATAGGTTAGACTTTAAGTCAATACTC-TTTTGATA-3') into the respective restriction sites to give the vector pCK\_T7. In order to clone genes for over-expression downstream of the T7AI promoter the restriction sites Bsp1407I and NdeI (sequences italicised) were included in the T7A1-up/dw primers so that the ribosome binding site was placed six nucleotides upstream of the ATG start codon (bold). In the final step the Mx8-phage derived *attP* site and *intP* were amplified from the vector pSWU105 (Dale Kaiser, unpublished) by employing the primers integrase\_for\_1 (5'-GGATGGATCTAGACAGACGGCCGCGCTTGT-3') and integrase\_rev\_1 (5'-CGGCTTTCGCGACATGGAGGACT-3'). The resulting PCR product was digested with XbaI and ligated into the PstI/XbaI digested vector to create the pCK\_T7A1\_att (for a map and nucleotide sequence of pCK\_T7A1\_att see Figures S1 and S2 in the Supporting Information).

The resulting *mvaS* complementation plasmid pCK4267exp was introduced into *M. xanthus* mutants DK5624 ( $\Delta bkd$ , *mvaS::kan*)<sup>[9]</sup> and HB015 ( $\Delta bkd$ , *MXAN\_4265::kan*) by electroporation as described previously;<sup>[14,46]</sup> this resulted in strains HB19 ( $\Delta bkd$ , *mvaS::kan*, *mvaS*<sup>+</sup>) and HB020 ( $\Delta bkd$ , *MXAN\_4265::kan*, *mvaS*<sup>+</sup>).

**Analytical procedures:** Fatty acids were analyzed as their methyl esters as described.<sup>[9]</sup> For geosmin analysis, a cell pellet from about 20 mL of culture was resuspended in methanol (500  $\mu$ L) and extracted with heptane (500  $\mu$ L) by being shaken at room temperature for 20 min. Samples were centrifuged to achieve phase separation, and an aliquot of the heptane phase (2  $\mu$ L) was injected into an Agilent 6890N gas chromatograph equipped with a 5973N EI-MS (Agilent, Waldbronn, Germany) by using a pulsed split-less injection technique. The column was an Agilent DB-5ht (30 m  $\times$  0.25 mm  $\times$  0.1  $\mu$ m), and the mobile phase was helium at 1 mL min<sup>-1</sup>. The GC inlet and GC-MS transfer-line temperatures were 250 °C and 280 °C, respectively. The column temperature was held at 90 °C for 5 min, then increased to 140 °C at 5 °C min<sup>-1</sup>, to 300 °C at 30 °C min<sup>-1</sup> at which it was held for 10 min, then decreased to 90 °C at 30 °C min<sup>-1</sup>. To improve sensitivity, the scan range of the MS was narrowed to *m/z* 50–200 with the sampling rate adjusted to achieve a scan rate of about 2.5 Hz. Identification and quantitation of geosmin and its isotopomers were done with the AMDIS software.

Analysis of Trypan blue binding to fibrils was performed as described previously.<sup>[37]</sup>

**Proteome analysis:** For proteome analysis, wild-type and *bkd* mutant cells (25 mL each) were grown in Erlenmeyer flasks (250 mL), and cells were harvested after 24 h at OD<sub>600</sub> 1.59 (DK1622) and OD<sub>600</sub> 1.52 for the *bkd*<sup>-</sup> culture (after 24 h). Therefore, the cultures were centrifuged (Eppendorf 5810R) at 3250 *g* at 4 °C for 10 min. The pellets were washed two times in 4 °C in cold PBS buffer and centrifuged under the same conditions. The cell pellets were stored at –20 °C.

For cell lysis, the pellets were resuspended in 2x lysis buffer (2 mL; 7 M urea, 2 M thiourea, 4% CHAPS (3-([3-cholamidopropyl]dimethylammonio)-1-propanesulfonate), 2% (v/v) pharmalyte 3–10, 2% DTT). Cell lysis was performed by using a French press (3 $\times$ ). The suspension was centrifuged and the supernatant was transferred to a new vial and proteins were precipitated with acetone/methanol.<sup>[50]</sup> The tube was incubated at –20 °C for 24 h and centrifuged as described above. The supernatant was removed quantitatively and the cell pellets were resuspended at 4 °C in 500–600  $\mu$ L DIGE label buffer (7 M urea, 2 M thiourea, 4% CHAPS, 30 mM Tris, pH 8.5). For the estimation of protein concentrations the Bradford protein assay was performed<sup>[51]</sup> with 1:10 and 1:20 dilutions of the samples and by using "Dye concentrate" (Biorad) and a microtiterplate reader (Bio-Tek EL808); samples were measured at 595 nm.

DIGE labelling<sup>[52]</sup> was performed at 4 °C in the dark. Each sample (50  $\mu$ g) was labelled with Cy3 or Cy5, and a 1:1 mixture (50  $\mu$ g) was labelled with Cy2 to generate the internal standard. After 30 min the labelling reaction was quenched by adding L-lysine (final concentration 1 mM). All samples were then pooled. We used the "under-labelling" technique, that is, both protein samples (150  $\mu$ g) without fluorescent labels were added to the mixture to ensure spots in Coomassie staining. Samples were loaded on dry strips (pH 3–11NL, Amersham) by following the manufacturer's instructions for in-gel-rehydration. We also applied each sample (500  $\mu$ g) to individual dry strips for conventional Coomassie gels. First dimension (isoelectric focusing), equilibration, and second dimension (SDS-PAGE) was performed as described previously.<sup>[53]</sup>

DIGE gels were scanned by using a THYPHOON 9410 (Amersham). For DIGE image analysis the DeCyder software package was used. DIGE spots that showed a different intensity higher than threefold in the comparison of the two samples were set to pick list. All gels were stained with colloidal Coomassie.<sup>[54]</sup> All Coomassie stained gels were scanned on a densitometer (ImageScanner, Amersham) and the images analyzed by IMAGE Master 5.0 (Swiss institute of bioinformatics). Coomassie spots that showed a different intensity higher than twofold in the comparison of the two samples were set to pick list, and all selected spots were cut out and subjected to in-gel-digestion as described previously.<sup>[53]</sup>

As matrix compound,  $\alpha$ -cyanocinnamic acid was dissolved to saturation in water/acetonitrile (1:1; 0.1% trifluoroacetic acid) and trypsin digests (2  $\mu$ L) were mixed with the matrix solution (2  $\mu$ L). An aliquot from this mixture (1–1.5  $\mu$ L) was spotted on a 384 MALDI Anchor chip® target plate (Bruker Daltonics) and dried at room temperature. Mass profiles were generated by using a MALDI ToF ULTRAFlex mass spectrometer (Bruker Daltonics), and covered a range from 800–3500 Da. Peak detection included SNAP algorithm, SN ratio higher than 25 and peptide-typical isotopic distribution. Mass spectra were automatically filtered for trypsin or keratin peaks. Optional C<sub>18</sub> ZipTips (Millipore) purification was used by following the manufacturer's instructions to purify and concentrated peptides. The elution was carried out with matrix solution (1.5  $\mu$ L) and spotted directly on the target plate.

The monoisotopic masses were transferred to MASCOT (Matrix Science) and the masses were analyzed by using the in-house database of the translated genome of *Myxococcus xanthus* DK1622. The search parameters were specified as follows: mass tolerance: "100 ppm", fixed modifications: "carbamidomethyl", variable modifications: "oxidized methionines", protease: "trypsin", missed cleavages: "0". The MOWSE scoring algorithm<sup>[55]</sup> identified proteins that had a score higher than 51, which corresponds to an identification probability of 95%.

**DNA microarrays:** The construction of the PCR-generated DNA microarrays that contained probes against the 7235 open reading frames of *M. xanthus*, has been previously described.<sup>[26,56,57]</sup> Processing of the DNA arrays, cDNA synthesis, microarray hybridization and posthybridization processing were performed as described.<sup>[58]</sup> Six independent biological replica pairs of DK1622 (wild type) and DK5643 ( $\Delta bkd$ ) were used for the analysis, and each independent wild type vs. *bkd* mutant pair was handled and processed identically. Briefly, each pair of strains was grown at 28 °C to a density of  $5 \times 10^8$  cells mL<sup>-1</sup>, the cells were centrifuged, the supernatants were removed, and the cell pellets were quick-frozen in liquid nitrogen. Total cellular RNA was isolated from quick-frozen cells by using the hot-phenol method.<sup>[59]</sup> Total RNA (30 µg) from matched cultures was used to synthesize cDNA with pdN6 primers (10 µg; Amersham Pharmacia) in the presence of RNase inhibitor (40 µg µL<sup>-1</sup>; Promega). Reverse transcriptase reaction times were modified as follows: 10 min at 37 °C, then 42 °C for 100 min, followed by a 10 min incubation at 50 °C. RNA was hydrolyzed and neutralized as described by Jakobsen et al.<sup>[26]</sup> and purified with Micron 30 filters (Amicon); the cDNA was eluted and dried with a SpeedVac concentrator (Savant). The dried cDNA was resuspended in sodium bicarbonate (0.1 M, pH 9.0; 9 µL), and incubated for 5 min at 37 °C. The cDNA was labelled with Cy3 (DK1622) or Cy5 (DK5643) from Amersham Pharmacia by addition of dye (2 µL) dissolved in dimethyl sulfoxide (10 µL) and incubated for 1 h in the dark. The labelled cDNA was purified with the QIA-quick PCR kit (Qiagen) as described by the manufacturer, and concentrated on a Micron 30 spin filter (Amicon). Labelled cDNA was then dried with a SpeedVac concentrator (Savant) and resuspended in hybridization buffer (45 µL). Hybridization and posthybridization processing of the slides were performed as described previously.<sup>[26,57,60]</sup>

Posthybridized DNA microarrays were scanned with a GenePix 4000A microarray scanner and read by using GenePix Pro 3.0 (Axon, Inc.). The GenePix array list (gal) file, MyxoGALv2.gal, that corresponded to the *M. xanthus* DNA microarrays, was constructed by using GalFileMaker v1.2 (DeRisi laboratory website; <http://derisi.lab.ucsf.edu>). Spots were flagged and removed from analyses based on stringent criteria for shape, signal intensity and background by using GenePix Pro 3.0 (Axon, Inc.). Analyses were performed with all unflagged spots. All array analyses, including hierarchical clustering and statistical analysis, were performed by using Cluster (Eisen Software; <http://rana.lbl.gov/EisenSoftware.htm>), Java TreeView software<sup>[61]</sup> (<http://sourceforge.net/projects/jtreeview>), and significance analysis of microarrays (SAM)<sup>[62]</sup> (<http://www-stat.stanford.edu/~tibs/SAM>). All DNA microarray results used for this study have been submitted to Gene Expression Omnibus (GEO) at NCBI (<http://www.ncbi.nlm.nih.gov/projects/geo/>). Series accession number: GSE10818; sample accession numbers: GSM273060, GSM273080, GSM273081, GSM273082, GSM273083, GSM273084.

**qRT-PCR analysis:** qRT-PCR of MXAN\_3757, MXAN\_3760, MXAN\_4263, MXAN\_4266, MXAN\_5020, MXAN\_5021 and MXAN\_5158 was performed as described previously with vegetative cultures of DK1622 and DK5643, with and without the addition of isovalerate (IVA; 1 mM).<sup>[9]</sup>

## Acknowledgements

*R.M. is grateful to the Deutsche Forschungsgemeinschaft for financial support. The authors would like to thank Taifo Mahmud for various helpful discussions during the course of this project*

*and W. Lorenzen for help with the GC/MS analyses. This work was in part supported by the National Institutes of Health Public Health Service grant GM354592 to M.S.*

**Keywords:** biosynthesis • isovaleryl-CoA • leucine degradation • *Myxococcus xanthus* • natural products

- [1] A. P. Bretscher, D. Kaiser, *J. Bacteriol.* **1978**, *133*, 763–768.
- [2] M. E. Diodati, R. E. Gill, L. Plamann, M. Singer in *Myxobacteria: Multicellularity and Differentiation* (Ed.: D. E. Whitworth), ASM, Washington, **2008**, pp. 43–76.
- [3] J. C. Ware, M. Dworkin, *J. Bacteriol.* **1973**, *115*, 253–261.
- [4] D. B. Kearns, A. Venot, P. J. Bonner, B. Stevens, G. J. Boons, L. J. Shimkets, *Proc. Natl. Acad. Sci. USA* **2001**, *98*, 13990–13994.
- [5] H. B. Bode, J. S. Dickschat, R. M. Kroppenstedt, S. Schulz, R. Müller, *J. Am. Chem. Soc.* **2005**, *127*, 532–533.
- [6] J. S. Dickschat, H. B. Bode, R. M. Kroppenstedt, R. Müller, S. Schulz, *Org. Biomol. Chem.* **2005**, *3*, 2824–2831.
- [7] D. R. Toal, S. W. Clifton, B. A. Roe, J. Downard, *Mol. Microbiol.* **1995**, *16*, 177–189.
- [8] G. Michal, *Biochemical Pathways*, Spektrum, Heidelberg, **1999**.
- [9] H. B. Bode, M. W. Ring, G. Schwär, R. M. Kroppenstedt, D. Kaiser, R. Müller, *J. Bacteriol.* **2006**, *188*, 6524–6528.
- [10] M. W. Ring, G. Schwär, V. Thiel, J. S. Dickschat, R. M. Kroppenstedt, S. Schulz, H. B. Bode, *J. Biol. Chem.* **2006**, *281*, 36691–36700.
- [11] J. Downard, D. Toal, *Mol. Microbiol.* **1995**, *16*, 171–175.
- [12] B. Silakowski, H. U. Schairer, H. Ehret, B. Kunze, S. Weinig, G. Nordsiek, P. Brandt, H. Blöcker, G. Höfle, S. Beyer, R. Müller, *J. Biol. Chem.* **1999**, *274*, 37391–37399.
- [13] B. Silakowski, G. Nordsiek, B. Kunze, H. Blöcker, R. Müller, *Chem. Biol.* **2001**, *8*, 59–69.
- [14] H. B. Bode, P. Meiser, T. Klefisch, N. Socorro D. J. Cortina, D. Krug, A. Göhring, G. Schwär, T. Mahmud, Y. A. Elnakady, R. Müller, *ChemBioChem* **2007**, *8*, 2139–2144.
- [15] B. Kunze, H. Reichenbach, R. Müller, G. Höfle, *J. Antibiot.* **2005**, *58*, 244–251.
- [16] T. Mahmud, H. B. Bode, B. Silakowski, R. M. Kroppenstedt, M. Xu, S. Nordhoff, G. Höfle, R. Müller, *J. Biol. Chem.* **2002**, *277*, 32768–32774.
- [17] T. Mahmud, S. C. Wenzel, E. Wan, K. W. Wen, H. B. Bode, N. Gaitatzis, R. Müller, *ChemBioChem* **2005**, *6*, 322–330.
- [18] J. A. Aguilar, A. N. Zavala, C. Díaz-Pérez, C. Cervantes, A. L. Díaz-Pérez, J. Campos-García, *Appl. Environ. Microbiol.* **2006**, *72*, 2070–2079.
- [19] K. Förster-Fromme, B. Höschle, C. Mack, M. Bott, W. Armbruster, D. Jendrosseck, *Appl. Environ. Microbiol.* **2006**, *72*, 4819–4828.
- [20] B. Höschle, V. Gnau, D. Jendrosseck, *Microbiology* **2005**, *151*, 3649–3656.
- [21] J. S. Dickschat, H. B. Bode, T. Mahmud, R. Müller, S. Schulz, *J. Org. Chem.* **2005**, *70*, 5174–5182.
- [22] H. B. Bode, S. C. Wenzel, H. Irschik, G. Höfle, R. Müller, *Angew. Chem.* **2004**, *116*, 4257–4262; *Angew. Chem. Int. Ed.* **2004**, *43*, 4163–4167.
- [23] H. B. Bode, B. Zeggel, B. Silakowski, S. C. Wenzel, H. Reichenbach, R. Müller, *Mol. Microbiol.* **2003**, *47*, 471–481.
- [24] J. S. Dickschat, S. C. Wenzel, H. B. Bode, R. Müller, S. Schulz, *ChemBioChem* **2004**, *5*, 778–787.
- [25] V. G. Tusher, R. Tibshirani, G. Chu, *Proc. Natl. Acad. Sci. USA* **2001**, *98*, 5116–5121.
- [26] J. S. Jakobsen, L. Jelsbak, R. D. Welch, C. Cummings, B. Goldman, E. Stark, S. Slater, D. Kaiser, *J. Bacteriol.* **2004**, *186*, 4361–4368.
- [27] S. Rachid, K. Gerth, I. Kochems, R. Müller, *Mol. Microbiol.* **2007**, *63*, 1783–1796.
- [28] B. S. Goldman, W. C. Nierman, D. Kaiser, S. C. Slater, A. S. Durkin, J. Eisen, C. M. Ronning, W. B. Barbazuk, M. Blanchard, C. Field, C. Halling, G. Hinkle, O. Iartchuk, H. S. Kim, C. Mackenzie, R. Madupu, N. Miller, A. Shvartsbeyn, S. A. Sullivan, M. Vaudin, R. Wiegand, H. B. Kaplan, *Proc. Natl. Acad. Sci. USA* **2006**, *103*, 15200–15205.
- [29] W. Buckel, U. Dorn, R. Semmler, *Eur. J. Biochem.* **1981**, *118*, 315–321.
- [30] W. Buckel, *Eur. J. Biochem.* **1986**, *156*, 259–263.
- [31] W. Buckel, H. Liedtke, *Eur. J. Biochem.* **1986**, *156*, 251–257.
- [32] J. Edmond, G. Popják, *J. Biol. Chem.* **1974**, *249*, 66–71.
- [33] T. Hao, D. Biran, G. J. Velicer, L. Kroos, *J. Bacteriol.* **2002**, *184*, 3348–3359.

- [34] D. Kaiser, *Annu. Rev. Microbiol.* **2004**, *58*, 75–98.
- [35] "Contact-Dependent Signaling in *Myxococcus xanthus*: The Function of the C-Signal in Fruiting Body Morphogenesis", L. Søgaard-Andersen in *Myxobacteria: Multicellularity and Differentiation*, (Ed.: D. E. Whitworth), ASM Press, Washington, **2008**, pp. 77–91.
- [36] A. Joachimiak, R. L. Kelley, R. P. Gunsalus, C. Yanofsky, P. B. Sigler, *Proc. Natl. Acad. Sci. USA* **1983**, *80*, 668–672.
- [37] W. P. Black, Z. Yang, *J. Bacteriol.* **2004**, *186*, 1001–1008.
- [38] "Secondary Metabolism in Myxobacteria", H. B. Bode, R. Müller in *Myxobacteria: Multicellularity and Differentiation*, (Ed.: D. Whitworth), ASM Press, Chicago, **2007**, pp. 259–282.
- [39] H. B. Bode, R. Müller, *Angew. Chem.* **2005**, *117*, 6988–7007; *Angew. Chem. Int. Ed.* **2005**, *44*, 6828–6846.
- [40] V. Simunovic, J. Zapp, S. Rachid, D. Krug, P. Meiser, R. Müller, *ChemBioChem* **2006**, *7*, 1206–1220.
- [41] P. Meiser, H. B. Bode, R. Müller, *Proc. Natl. Acad. Sci. USA* **2006**, *103*, 19128–19133.
- [42] S. C. Wenzel, P. Meiser, T. Binz, T. Mahmud, R. Müller, *Angew. Chem.* **2006**, *118*, 2354–2360; *Angew. Chem. Int. Ed.* **2006**, *45*, 2296–2301.
- [43] C. Schley, M. O. Altmeyer, R. Swart, R. Müller, H. CG, *J. Proteome Res.* **2006**, *5*, 2760–2768.
- [44] D. Kaiser, *Proc. Natl. Acad. Sci. USA* **1979**, *76*, 5952–5956.
- [45] J. Hodgkin, D. Kaiser, *Proc. Natl. Acad. Sci. USA* **1977**, *74*, 2938–2942.
- [46] H. B. Bode, M. W. Ring, D. Kaiser, A. C. David, R. M. Kroppenstedt, G. Schwär, *J. Bacteriol.* **2006**, *188*, 5632–5634.
- [47] T. M. Binz, S. C. Wenzel, H. J. Schnell, A. Bechthold, R. Müller, *ChemBioChem* **2008**, *9*, 447–454.
- [48] S. C. Wenzel, F. Gross, Y. Zhang, J. Fu, F. A. Stewart, R. Müller, *Chem. Biol.* **2005**, *12*, 349–356.
- [49] J. P. Muyrers, Y. Zhang, A. F. Stewart, *Genet. Eng. (NY)* **2000**, *22*, 77–98.
- [50] R. Mastro, M. Hall, *Anal. Biochem.* **1999**, *273*, 313–315.
- [51] M. M. Bradford, *Anal. Biochem.* **1976**, *72*, 248–254.
- [52] R. Tonge, J. Shaw, B. Middleton, R. Rowlinson, S. Rayner, J. Young, F. Pognan, E. Hawkins, I. Currie, M. Davison, *Proteomics* **2001**, *1*, 377–396.
- [53] S. Schneiker, O. Perlova, O. Kaiser, K. Gerth, A. Alici, M. O. Altmeyer, D. Bartels, T. Bekel, S. Beyer, E. Bode, H. B. Bode, C. J. Bolten, J. V. Choudhuri, S. Doss, Y. A. Elnakady, B. Frank, L. Gaigalat, A. Goesmann, C. Groeger, F. Gross, L. Jelsbak, L. Jelsbak, J. Kalinowski, C. Kegl, T. Knauber, S. Konietzny, M. Kopp, L. Krause, D. Krug, B. Linke, T. Mahmud, R. Martinez-Arias, A. C. McHardy, M. Meraj, F. Meyer, S. Mormann, J. Munoz-Dorado, J. Perez, S. Pradella, S. Rachid, G. Raddatz, F. Rosenau, C. Ruckert, F. Sasse, M. Scharfe, S. C. Schuster, G. Suen, A. Treuner-Lange, G. J. Velicer, F. J. Vorholter, K. J. Weissman, R. D. Welch, S. C. Wenzel, D. E. Whitworth, S. Wilhelm, C. Wittmann, H. Blöcker, A. Pühler, R. Müller, *Nat. Biotechnol.* **2007**, *25*, 1281–1289.
- [54] R. Westermeier, *Proteomics* **2006**, *6 Suppl 2*, 61–64.
- [55] D. J. C. Pappin, P. Hojrup, A. J. Bleasby, *Curr. Biol.* **1993**, *3*, 327–332.
- [56] M. E. Diodati, F. Ossa, N. B. Caberoy, I. R. Jose, W. Hiraiwa, M. M. Igo, M. Singer, A. G. Garza, *J. Bacteriol.* **2006**, *188*, 1733–1743.
- [57] V. D. Pham, C. W. Shebelut, M. E. Diodati, C. T. Bull, M. Singer, *Microbiology* **2005**, *151*, 1865–1874.
- [58] M. E. Diodati, F. Ossa, N. B. Caberoy, I. R. Jose, W. Hiraiwa, M. M. Igo, M. Singer, A. G. Garza, *J. Bacteriol.* **2006**, *188*, 1733–1743.
- [59] J. Sambrook, E. F. Fritsch, T. Maniatis, *Molecular Cloning: A Laboratory Manual*, Cold Spring Harbor Laboratory Press, New York, **1989**.
- [60] M. E. Diodati, F. Ossa, N. B. Caberoy, I. R. Jose, W. Hiraiwa, M. M. Igo, M. Singer, A. G. Garza, *J. Bacteriol.* **2006**, *188*, 1733–1743.
- [61] A. J. Saldanha, *Bioinformatics* **2004**, *20*, 3246–3248.
- [62] V. G. Tusher, R. Tibshirani, G. Chu, *Proc. Natl. Acad. Sci. USA* **2001**, *98*, 5116–5121.

---

Received: April 3, 2008

Published online on ■ ■ ■, 2008

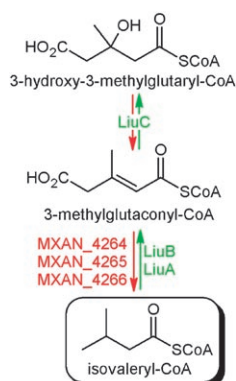
## FULL PAPERS

H. B. Bode, M. W. Ring, G. Schwär,  
M. O. Altmeyer, C. Kegler, I. R. Jose,  
M. Singer, R. Müller\*

■ ■ - ■ ■



**Identification of Additional Players in the Alternative Biosynthesis Pathway to Isovaleryl-CoA in the Myxobacterium *Myxococcus xanthus***



**Keeping your options open:** Two operons harbouring the genes that govern the alternative biosynthesis pathway to isovaleryl-CoA (red) and its reverse counterpart (green) have been identified in the myxobacterium *Myxococcus xanthus* by using a comparative transcriptome experiment and a set of feeding studies. This novel biosynthetic pathway branches off from the well-known mevalonate-dependent isoprenoid biosynthesis route.